NANO LETTERS

LETTER

pubs.acs.org/NanoLett

Quantum Transport in Graphene Nanonetworks

Andrés R. Botello-Méndez,[*,†] Eduardo Cruz-Silva,[‡] José M. Romo-Herrera,[§] Florentino López-Urías,[∥] Mauricio Terrones,[⊥,#] Bobby G. Sumpter,[‡,▽] Humberto Terrones,[†,‡] Jean-Christophe Charlier,[†] and Vincent Meunier[¶]

[†]Institute of Condensed Matter and Nanosciences (IMCN), Université catholique de Louvain (UCL), Chemin des Etoiles 8, bte L7.03.01, 1348 Louvain-la-Neuve, Belgium

[‡]Center for Nanophase Materials Sciences and [▽]Computer Science & Mathematics Division, Oak Ridge National Laboratory, One Bethel Valley Road, Oak Ridge, Tennessee 37831-6367, United States

[§]Departamento de Química Física and Unidad Asociada CSIC, Universidad de Vigo, 36310 Vigo, Spain

[∥]IPICYT, Camino a la presa San José 2055, 78216 San Luis Potosí, Mexico

[⊥]Research Center for Exotic Nanocarbons, Shinshu University, Wakasato 4-17-1, Nagano-city 380-8553, Japan

[¶]Department of Physics, Applied Physics, and Astronomy, Rensselaer Polytechnic Institute, 110 Eighth Street, Troy, New York 12180-3590, United States

[#]Department of Physics and Materials Research Institute, The Pennsylvania State University, 104 Davey Lab., University Park, Pennsylvania 16802-6300, United States

ABSTRACT: The quantum transport properties of graphene nanoribbon networks are investigated using first-principles calculations based on density functional theory. Focusing on systems that can be experimentally realized with existing techniques, both in-plane conductance in interconnected graphene nanoribbons and tunneling conductance in out-of-plane nanoribbon intersections were studied. The characteristics of the ab initio electronic transport through in-plane nanoribbon cross-points is found to be in agreement with results obtained with semiempirical approaches. Both simulations confirm the possibility of designing graphene nanoribbon-based networks capable of guiding electrons along desired and predetermined paths. In addition, some of these intersections exhibit different transmission probability for spin up and spin down electrons, suggesting the possible applications of such networks as spin filters. Furthermore, the electron transport properties of out-of-plane nanoribbon cross-points of realistic sizes are described using a combination of first-principles and tight-binding approaches. The stacking angle between individual sheets is found to play a central role in dictating the electronic transmission probability within the networks.

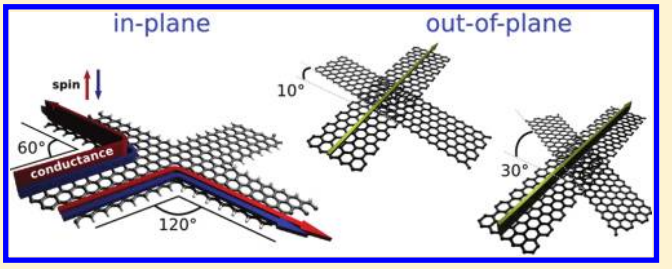

KEYWORDS: Graphene, graphene nanoribbons, quantum transport, bilayer graphene, spin transport

Graphene exhibits remarkable electronic properties that are responsible for unusual physics due to the pseudorelativistic behavior of its low-energy electrons.[1] For instance, graphene possesses record-high electronic mobilities, can support large current densities, and exhibits unusually high thermal conductivity.[1] These properties place graphene as one of the most attractive materials for electronic applications. However, graphene is a zero gap semiconductor and consequently cannot be directly introduced as a material for mainstream logic electronic devices. The absence of an electronic gap makes it a poor candidate to achieve a sufficiently large I_{ON} to I_{OFF} ratio needed for practical logic device operation. Fortunately, a gap can be induced in a number of ways. For instance, structural alterations of the two-dimensional (2D) graphene sheet can effectively reduce the system's dimensionality and lead to one-dimensional (1D) graphene nanoribbons (GNRs), a material with appealing electronic properties such as a clear gap at the Fermi level. These one-atom thick one-dimensional graphitic strips offer great promise for future nanoelectronic applications.[2] In fact, this prediction has been realized by theoretical studies well before the experimental isolation of graphene.[3,4] GNRs are characterized by pronounced electronic confinement.[5] Notably, very narrow GNRs (<5 nm)[6] with well-defined edges, that is, without topological disorder at the atomic scale, are needed to achieve practical gaps (~0.4 eV).

The controlled formation of narrow graphene strips with well-defined edges has been an intense topic of research. Significant progress in this direction has been achieved recently, as described in recent reviews.[7,8] Well-defined crystallographic edges with zigzag or armchair morphologies are products of CVD-grown graphene inside a TEM after processing using Joule heating,[9] or

Received: January 20, 2011
Revised: June 6, 2011
Published: June 22, 2011

dx.doi.org/10.1021/nl2002268 | *Nano Lett.* 2011, 11, 3058–3064

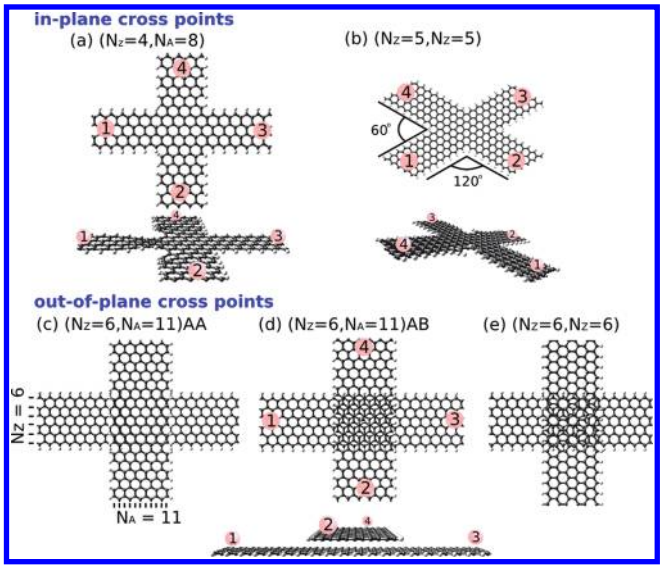

Figure 1. Ball and stick models of the different in-plane (a,b) and out-of-plane (c−e) conducting GNR networks. Notice the atomic reconstruction induced by neighboring hydrogen atoms at the intersection of the in-plane GNR networks, obtained after ab initio structural optimization.

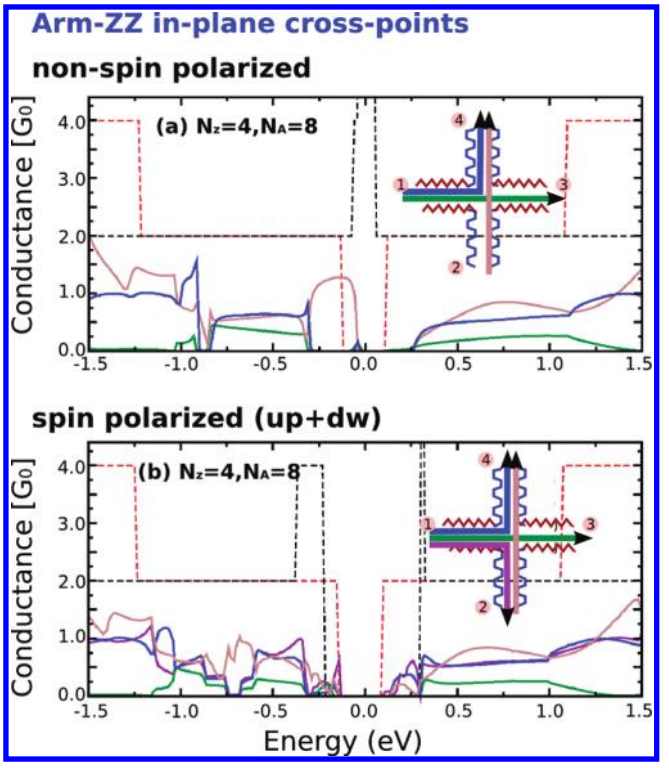

Figure 2. (a) Nonspin polarized and (b) spin polarized (sum of spin up and spin down contributions) quantum conductance along nonequivalent paths in the in-plane cross-points between an armchair ($N_A = 8$) and a zigzag ($N_Z = 4$) graphitic nanoribbon. In (a), the dashed black (red) line corresponds to the paramagnetic state conductance in the isolated Z-GNR (A-GNR). In (b) the black and red lines refer to the total conductance (spin up + spin down) of the isolated Z-GNR (antiferromagnetic state) and A-GNR (paramagnetic state).

can be obtained from graphene by scanning tunneling lithography,[10] or through catalytic cutting.[11,12] Large scale synthesis of GNRs from the unzipping of carbon nanotubes (CNTs) along their axis has also been demonstrated.[7,13] Unzipping can be achieved by plasma etching of single-wall carbon nanotubes to yield very narrow nanoribbons.[14−16] The use of CNTs as starting material to produce GNRs presents the advantage that all the already available technology of CNT production can be exploited for the realization of practical GNR-based electronic elements. For instance, it has been demonstrated that arrays and networks of CNTs can be used to produce well-aligned arrays and networks of GNRs.[15] Even though the edges of such nanoribbons are not atomically smooth, devices constructed with arrays of nanoribbons display relatively high I_{ON} to I_{OFF} ratio. In addition, a recent study based on the bottom-up fabrication of GNRs from the dehalogenation and cyclodehydrogenation of self-assembled polyphenylenes confirms the promise of a controlled synthesis of GNRs-based nanonetworks.[17]

In this Letter, the quantum transport properties of in-plane and out-of-plane multiterminal GNR assemblies are investigated using various computational methods. The ab initio quantum conductance calculations across geometrically relaxed in-plane cross-points presented here confirm previous results obtained using semiempirical approaches.[18,19] Out-of-plane GNR cross-points are investigated with a combination of ab initio and semiempirical techniques, showing the importance of the relationship between the stacking angle between the nanoribbons on the transmission of electrons. In principle, the first type of cross-point (Figure 1a,b) can be achieved experimentally from standard lithography, scanning tunneling lithography,[10] catalytic cutting,[11] from bottom-up chemical routes,[17] or using scalable approaches based on porous templates.[20] Out-of-plane cross-points (Figure 1c−e) can be obtained from an aligned array of CNTs, as has already been demonstrated experimentally.[15]

Models of GNR cross-points consist of graphene networks satisfying periodic boundary conditions. These networks are constructed from both zigzag and armchair GNRs containing different number of zigzag chains (N_Z), and different number of dimer chains (N_A) along their width (Figure 1). Calculations were performed using density functional theory (DFT)[21,22] as implemented in the SIESTA code.[23] The generalized gradient approximation (GGA) with the PBEsol parametrization[24] was chosen for the exchange-correlation functional. In order to deal with the large number of atoms in the unit cells (∼500), norm-conserving pseudopotentials,[25] as well as a numerical localized combination of atomic orbitals (double-ζ basis) were used to expand the wave functions. The Brillouin zone was integrated with a 2 × 2 × 1 Monkhorst-Pack grid and a 100 Ry mesh was used as cutoff for the integration in the 3D real space grid. The geometries were relaxed until the amplitude of the forces on each atom was less than 0.05 eV/Å . The self-consistent Hamiltonian and overlap matrices corresponding to the converged densities were then extracted to compute the quantum conductance properties within the framework of the Landauer−Büttiker formalism, and the surface Green's function matching method.[26,27]

Figure 1a shows the atomic structure of a cross-point between the $N_Z = 4$ and $N_A = 8$ GNRs. The effects of geometric relaxation are evident in the side view, where several atoms were displaced out-of-plane, due to the presence of two neighboring hydrogen atoms on both sides of the cross. An analogous atomic rearrangement is observed in a cross-point between two $N_Z = 5$ GNRs (Figure 1b). Note that such atomic reconstruction will always be present at cross-points between two zigzag nanoribbons with the

dx.doi.org/10.1021/nl2002268 |Nano Lett. 2011, 11, 3058–3064

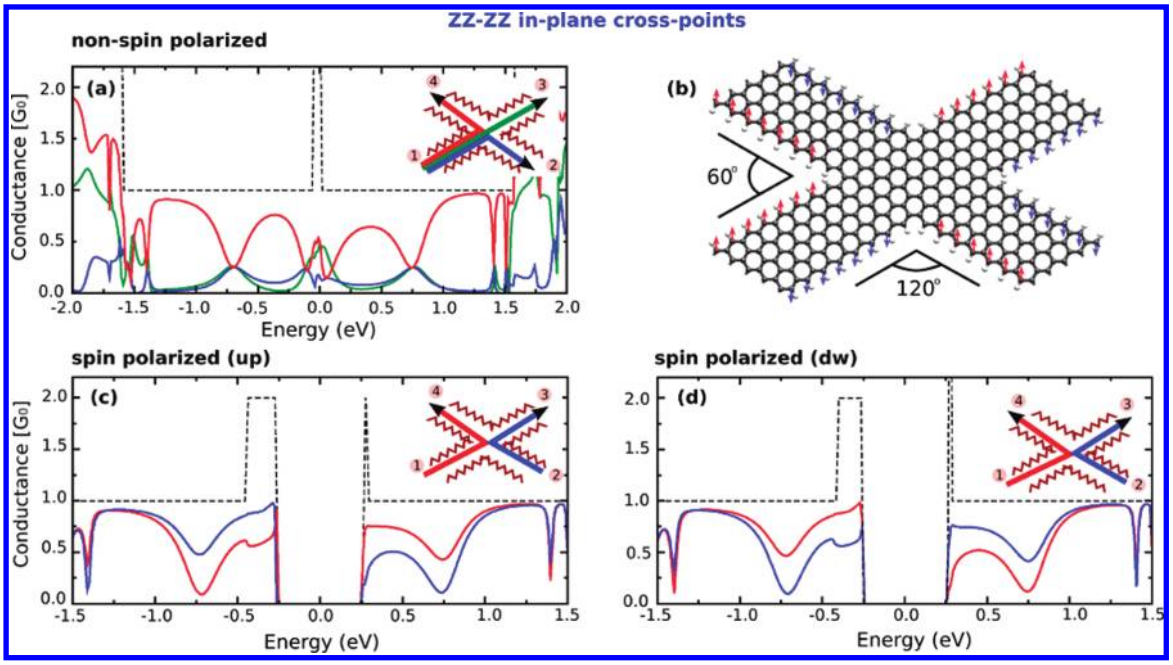

Figure 3. (a) Quantum conductance of an in-plane cross-point between two Z-GNRs for various transmission paths (paramagnetic state). (b) Ball and stick representation of the Z-GNR intersection between $N_Z = 5$ and $N'_Z = 5$ used in the calculations. The blue and red arrows represent the spin configuration corresponding to the curves shown in (c,d). (c,d) Spin polarized quantum conductance of a Z-GNR as represented in (b). Note the different spin-up and spin-down transmission probabilities along the same path (e.g., 1−4). While the total transmission (spin up + spin down) is symmetric along various paths, the spin state effectively breaks the structure's symmetry (i.e., vertical C_2 axis), yielding a spin-dependent conductance. The dashed black line represents the conductance of an isolated Z-GNR in the corresponding spin-state.

same number of zigzag chains, while it can be avoided in cross-points between GNRs with different types of edges by choosing appropriate widths (i.e., with even values for N_A). An alternative reconstruction would necessitate the presence of nonhexagonal rings at these junctions, as observed experimentally under a transmission electron microscope.[28]

The electronic transport properties of isolated GNRs are sensitive to the shape of the edges and the width of the ribbon.[6] A-GNRs exhibit a band gap E_g that decreases with the width. Consequently, a region of zero conductance is observed in A-GNRs due to the absence of electronic channels in the energy window around E_g. For instance, the dashed red line in Figure 2a displays the conductance across an isolated A-GNR with $N_A = 8$. Conversely, the electronic band structure of Z-GNRs exhibits localized edge states close to the Fermi energy (E_F). The states extend along the edges and correspond to nonzero density of states at E_F and a high electronic conductance at the charge neutrality point (dashed black line in Figure 2a). Spin polarized calculations reveal that such edge states carry a finite magnetic moment with a ferromagnetic ordering along the edges but an antiferromagnetic ordering between them.[29] The interaction between the edges leads to a magnetic insulating ground state. The edge interaction and the band gap decrease with the GNR's width. As the width of the Z-GNR increases, such interaction weakens, and the difference in energy between the parallel and antiparallel spin ordering along the edges disappears. Therefore, the spin polarized electron conductance of a narrow Z-GNR exhibits zero conduction around the charge neutrality point, and two sharp peaks of conductance due to the presence of edge states (see the dashed black curve of Figure 2b)

The electron conduction at low energies in a Z-GNR proceeds mainly along its edges, thus, it is expected to be significantly reduced by reflections if the edges are interrupted, as shown in Figure 2a,b (1−3) for an in-plane cross-point with different ($N_Z = 4$, $N_A = 8$) edge geometries. In contrast, for a continuous zigzag edge, as in the ($N_Z = 5$, $N_A = 5$) please cross-point (see Figure 3), the electronic transport through consecutive leads exhibits only minor scattering (e.g., 1−4, in Figure 3a). The conduction is significantly larger for a zigzag edge making a 60° angle compared with that making a 120° angle. Similar behavior is observed in spin-polarized calculations.

The conductance between a Z-GNR and an A-GNR exhibits a sharp decrease in conduction due to the existence of a gap in the A-GNR system. It also exhibits significant scattering due to band mixing and is very sensitive to the geometry of the intersection. Along an A-GNR, the introduction of branches results in a reduction in conductance due to the band mixing at the intersection (Figure 2a (2−4)). Comparing the nonspin and spin-polarized calculations (Figure 2a,b (2−4)), we clearly see that the energy position of the zigzag edge state is important since such states enhance the band-mixing and scattering of the transport along the A-GNR.

The conductance across continuous or in-plane networks of GNRs has already been investigated using a simple single-orbital nearest-neighbor tight-binding method.[18,19] In agreement with these results, the transport properties of in-plane cross-points are found to be very sensitive to the geometry of the junction. Notably, under such an approximation, which does not consider spin degrees of freedom nor relaxation of the atomic positions, the conductance along a Z-GNR and across a cross-point exhibits high conductance ($\sim 0.8 G_0$).[18] In contrast, the ab initio results obtained in the present work indicate that the electronic transport properties of GNRs are significantly affected when they are assembled into networks or branches. A notable exception is the

dx.doi.org/10.1021/nl2002268 |Nano Lett. 2011, 11, 3058–3064

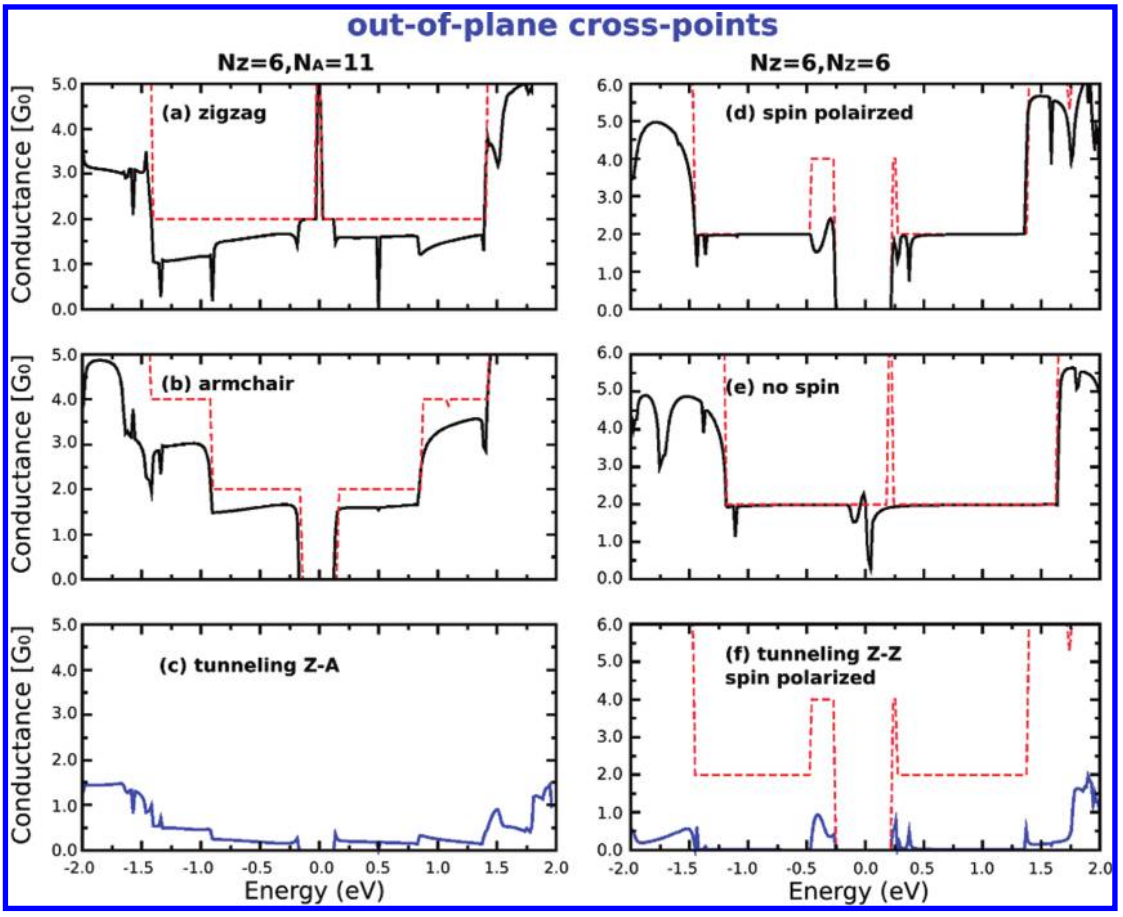

Figure 4. Quantum conductance through out-of-plane or bilayer GNR networks formed from using two intersecting A-GNR and a Z-GNR (left) with AB stacking, and two Z-GNRs (right). The dashed lines represent the conductance of isolated GNRs. Notice that the small tunneling current between the GNRs depends on the type of intersection and the localization of the electrons at a particular energy (e.g., edge states).

cross-point between two Z-GNRs terminals forming an angle of 60° in which the scattering is minimal as illustrated in Figure 3a,c, d (1−4) or (2−3). Note that this phenomenon was already pointed out in a tight-binding study of GNRs with turns.[19] However, the first principles spin-polarized calculations presented here reveal that these 60° intersections have interesting spin transmission behavior. In order to comply with the periodic boundary conditions, the most stable configuration (shown in Figure 3b) exhibits different spin alignment at the edges of the two 60° turns at the intersection. The existence of the antiferromagnetic state combined with the presence of the junction effectively break the left-right symmetry (Figure 3b). As a consequence, the transmission probability is different for the two spin channels. For instance, the low energy spin up electron conductance along the 1−4 is significantly higher than the spin down conductance along this path (compare the red lines in Figure 3c,d). Opposite behavior is observed for the 2−3 paths. However, note that the symmetric pathways in the total conductance is retrieved (the sum of spin up and spin down contribution).

An alternative arrangement for GNR networks is through out-of-plane or bilayer cross-points. In these cases, the interaction between the two GNRs is weak, and the changes in conductance across the GNRs and the conductance between them are driven by tunneling across the GNR cross-point. As illustrated in Figure 4, this hypothesis is confirmed by the ab initio quantum conductance along and across the different GNRs shown in Figure 1c−e. At the cross-point between an A-GNR and Z-GNRs (Figure 1d), the conductance along the A-GNR is reduced to ∼75% (Figure 4b). A similar decrease is observed for the conductance across the Z-GNR (Figure 4a), with the notable exception of the energy range around the charge neutrality point, where the conductance is mainly due to the edge states, indicating that the edge states do not tunnel to the A-GNR. Indeed, the loss of transmitted electrons through tunneling at a cross-point between two Z-GNRs is almost nonexistent, regardless of their spin polarizations, as shown in Figure 4c,f. For the case of a cross-point between two Z-GNRs, there is very little tunneling at the one electron channel (Figure 4d,e). Only the electrons localized at the edges tunnel across the GNRs (Figure 4f).

First-principles calculations are limited by computational resources to investigate routinely the transport properties of realistic nanoribbons, which include a much larger number of atoms than in the systems studied above. For this reason, a single-band tight-binding (TB) model using a Slonzcewski−Weiss−McClure (SWMC)-like parametrization[30] is proposed to investigate larger systems. In order to describe accurately the properties of graphene and GNRs, interactions up to the third nearest-neighbor[31] are considered by setting a cutoff interaction of 3.7 Å, and an exponential decay of the hopping parameter of the form $e^{(-\eta(d-d_0))}$, where d is the separation between two carbon atoms, and d_0 is the C−C equilibrium distance (1.42 Å for in-plane

dx.doi.org/10.1021/nl2002268 |Nano Lett. 2011, 11, 3058–3064

Table 1. Third Nearest-Neighbor Tight-Binding Parameters: Hopping Integrals (γ in eV), Decay Constants (η in Å^{-1}), and on-Site Energies (ε in eV)

$\gamma_0^{\alpha\alpha}$	$\gamma_0^{\alpha_A\alpha_B}$	$\gamma_0^{\delta\delta}$	$\gamma_0^{\delta\alpha}$	γ_1
−2.53	−3.35	−3.93	−3.35	0.32
$\eta_0^{\alpha\alpha}$	$\eta_0^{\alpha_A\alpha_B}$	$\eta_0^{\delta\delta}$	$\eta_0^{\delta\alpha}$	η_1
2.99	1.35	3.00	1.83	7.46
ε_α^Z		ε_α^A		ε_δ^A
−0.16		−0.5		−1.0

interactions, and 3.35 Å for out-of plane interactions). Different hopping parameters (γ_0) were used for the α_A and α_B sites of the carbon hexagonal lattice in graphene. In order to properly describe the band gap of A-GNRs, corrections to the on-site (ε_δ) and hopping parameters of edge atoms (γ^δ) and their interaction with other atoms are included as suggested in ref 32. One parameter is used for the out-of-plane interactions (γ_1). In order to align the Fermi level of A- and Z-GNRs, different on-site energies are needed. Starting from this model, the numerical values of the on-site and hopping parameters were fine-tuned using an evolutionary algorithm. The fitness function was defined as a weighted error of the calculated band structure with respect to the first-principles DFT-PBEsol band structure calculations. The weight was chosen to minimize the error at low energies. The ab initio band structures of graphene, GNRs, bilayer graphene, and GNR networks were used as references. The list of resulting tight-binding parameters are summarized in Table 1.

The results obtained using TB and DFT for the $N_A = 11$ $N_Z = 6$ GNR cross-point with AB stacking are compared in Figure 5a, confirming a satisfactory agreement in the energy region close to the charge neutrality point.

The calculated quantum conductance of the 5 nm wide GNRs are presented in Figure 5b. The conductance through a cross-point between the A-GNR and Z-GNR with AB stacking shows a significant loss of conductance along the GNR. In particular, the conductance along the GNRs is reduced to ∼25% compared to the conductance of the corresponding isolated GNRs. Remarkably, however, electrons in the edge state channels do not tunnel away significantly in agreement with the ab initio results presented above.

Bilayer graphene has been proposed as an alternative for future carbon-based electronics since a gap can be tuned using an external electric field.[33] Out-of-plane GNR cross-points are locally equivalent to bilayer graphene. Consequently, the effect of an external electric field in such cross-points has been studied using a TB model with modified on-site energies for one GNR. This approach induces a relative shift of the two GNR Fermi energies. Figure 5c presents the electronic transport of this out-of-plane GNR cross-point for positive and negative bias potentials. At a negative bias of −0.4 eV, the edge states of the Z-GNR are located within the energy of the one-electron channel of the A-GNR, where tunneling from the A-GNR to the Z-GNR occurs, thus suggesting that if the edge states are available, the electrons on the A-GNR will tunnel to the Z-GNR, leaving behind dips in the conductance along the A-GNR.

DFT calculations within the GGA approximation are known to underestimate the weak attraction between graphene layers.[34] However, the exponential decay of the TB approach presented

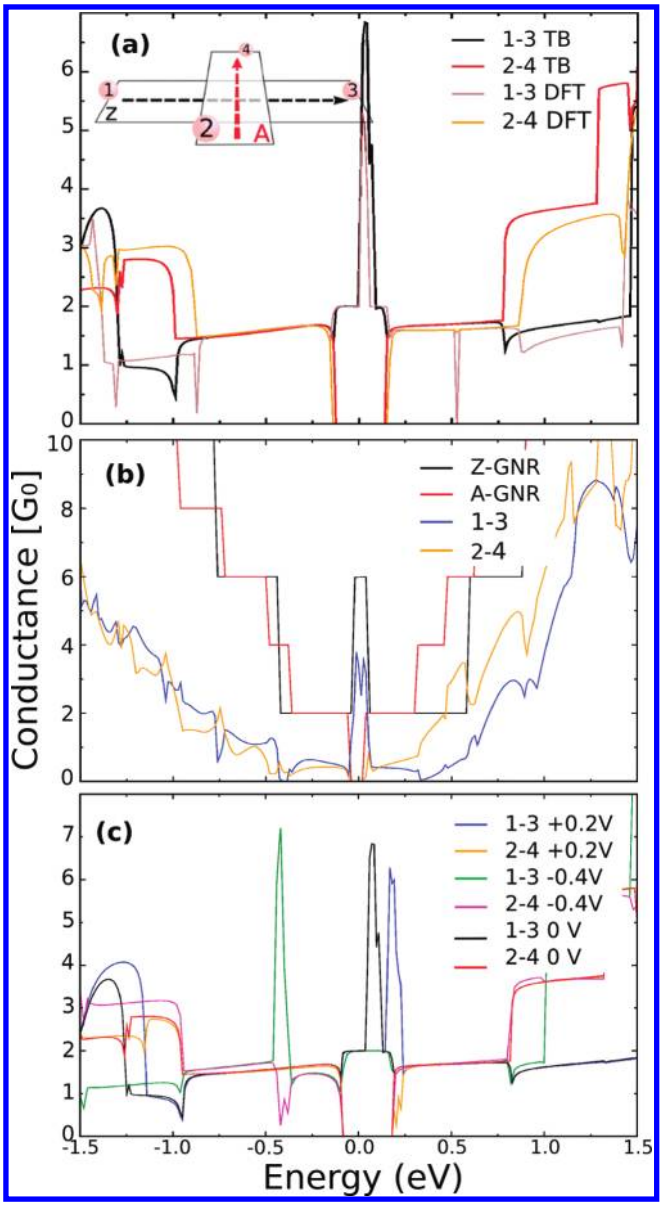

Figure 5. (a) Quantum conductance through an out-of-plane GNR cross-point with $N_A = 11$ and $N_Z = 6$ calculated using both TB and DFT approaches for the sake of comparison. (b) Quantum conductance of a GNR cross-point with a realistic width of ∼5 nm. c) Changes in quantum conductance across armchair and zigzag nanoribbons under a vertical electric field of various strengths.

here can successfully model the difference of interaction between the AA (Figure 1d) and AB (Figure 1c) stacking within GNR cross-points. In fact, the top down approach proposed in ref 15 and probably any other approach has little or no control on the way two nanoribbons are stacked. The effect of different stacking order has been investigated using the present tight-binding approach. The separation between the layers was fixed to 3.35 Å which corresponds to the experimental values of the AB stacking in graphite. Starting from a cross-point as depicted in Figure 1d, the armchair nanoribbon is rotated by an angle θ as described in Figure 6a. The conductance along and across the nanoribbons are likely to strongly depend on the stacking angle θ. Figure 6c shows the conductance at ±0.5 eV as a function of the stacking

dx.doi.org/10.1021/nl2002268 |*Nano Lett.* 2011, 11, 3058–3064

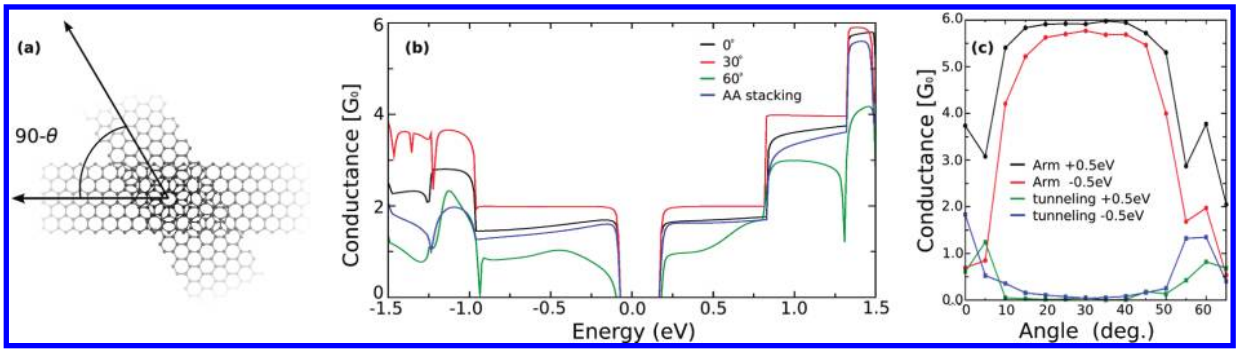

Figure 6. Quantum conductance through a A-GNR/Z-GNR out-of-plane GNR cross-point as a function of the stacking angle θ. (a) Atomic model depicting the A-GNR and the Z-GNR intersecting at 30°. (b) Conductance along an A-GNR in a $N_A = 11$ $N_Z = 6$ cross-point for various intersection angles compared to the AA stacking. (c) Quantum conduction as a function of the stacking angle θ for a A-GNR − Z-GNR cross-point with a ∼5 nm width.

angle θ both along an A-GNR, and from an A-GNR to an Z-GNR each with a width of ∼5 nm. A maximum of conductance along the A-GNR is observed for θ values around 30° with almost a 10-fold increase compared to its value at $\theta = 0°$ for −0.5 eV. This increase is due to the fact that the interaction between the GNRs is minimal at $\theta = 30°$. Conversely, at $\theta \gg 30°$, the overlap and interaction between the GNRs increase, thus enhancing the tunneling probability and increasing the scattering in the isolated GNR. A similar behavior is observed for different energies for selected stacking angles (Figure 6b). The direct comparison between the AA and AB stacking is also presented in Figure 6b, for a $N_A = 11$, $N_Z = 6$ intersection, suggesting that the effect of different stacking orders at $\theta = 0°$ has less impact on the conductance than the stacking angle.

In conclusion, first-principles and tight-binding calculations were performed on a number of GNR cross-points, and their quantum transport properties were computed. The simulations presented here indicate that GNR networks are appealing for potential applications and could play an important role in the development of carbon-based electronics. The quantum transport through in-plane GNR cross-points is found to be severely scattered at the intersections, except for 60° Z-GNR terminals, confirming the idea suggested before[19] that patterned graphene and GNRs could be used for functional devices and current flux guides.[35] In addition, the transmission probability at these intersections is different for spin up and spin down electrons, suggesting the possibility of their use as spin filters. Furthermore, the tunneling transmission at the intersection of bilayer GNR networks is predicted to be very sensitive to the stacking angle between the ribbons. The edge state channels are remarkably robust and could be tuned with an external electric field in order to induce tunneling from an A-GNR, thus allowing future development in band to band tunneling GNR-based transistors.[36] Finally, the present theoretical work suggests the importance of the ribbon edges, thus confirming the pressing need for improved scalable methods for the synthesis of GNR with atomically clean edges.[37]

AUTHOR INFORMATION

Corresponding Author

*E-mail: andres.botello@uclouvain.be.

ACKNOWLEDGMENT

A.R.B.M. is indebted to the *M. De Merre* Prize of Louvain. Parts of this work are directly connected to the F.R.S.-FNRS of Belgium, the Belgian PAI6 Program on "Quantum Effects in Clusters and Nanowires", and to the ARC project on "Graphene". B.G.S. and E.C.S. were supported by the Center for Nanophase Materials Sciences (CNMS) at Oak Ridge National Laboratory, sponsored by the Scientific User Facilities Division, U.S. Department of Energy. J.M.R-H. acknowledges the *Juan de la Cierva* fellowship from Ministerio de Ciencia e Innovación from Spain. M.T. thanks JST-Japan for funding the Research Center for Exotic NanoCarbons under the Japanese regional Innovation Strategy Program by the Excellence. H.T. acknowledges the Ecole Polytechnique of Louvain and CNMS ORNL for their support as visiting professor.

REFERENCES

(1) Neto, A. H. C.; Guinea, F.; Peres, N. M. R.; Novoselov, K. S.; Geim, A. K. *Rev. Mod. Phys.* **2009**, *81*, 109–54.
(2) Geim, A. K.; Novoselov, K. S. *Nat. Mater.* **2007**, *6*, 183–191.
(3) Nakada, K.; Fujita, M.; Dresselhaus, G.; Dresselhaus, M. S. *Phys. Rev. B* **1996**, *54*, 17954.
(4) Novoselov, K. S.; Geim, A. K.; Morozov, S. V.; Jiang, D.; Zhang, Y.; Dubonos, S. V.; Grigorieva, I. V.; Firsov, A. A. *Science* **2004**, *306*, 666–669.
(5) Dubois, S. M.; Zanolli, Z.; Declerck, X.; Charlier, J.-C. *Eur. Phys. J. B* **2009**, *72*, 1–24.
(6) Yang, L.; Park, C.; Son, Y.; Cohen, M. L.; Louie, S. G. *Phys. Rev. Lett.* **2007**, *99*, 186801.
(7) Terrones, M.; Botello-Méndez, A. R.; Campos-Delgado, J.; López-Urías, F.; Vega-Cantú, Y. I.; Rodríguez-Macías, F. J.; Elías, A. L.; Muñoz-Sandoval, E.; Cano-Márquez, A. G.; Charlier, J.-C.; Terrones, H. *Nano Today* **2010**, *5*, 351–372.
(8) Jia, X.; Campos-Delgado, J.; Terrones, M.; Meunier, V.; Dresselhaus, M. S. *Nanoscale* **2011**, *3*, 86–95.
(9) Jia, X.; Hofmann, M.; Meunier, V.; Sumpter, B. G.; Campos-Delgado, J.; Romo-Herrera, J. M.; Son, H.; Hsieh, Y.; Reina, A.; Kong, J.; Terrones, M.; Dresselhaus, M. S. *Science* **2009**, *323*, 1701–1705.
(10) Tapaszto, L.; Dobrik, G.; Lambin, P.; Biro, L. P. *Nat. Nanotechnol.* **2008**, *3*, 397–401.
(11) Ci, L.; Xu, Z.; Wang, L.; Gao, W.; Ding, F.; Kelly, K. F.; Yakobson, B. I.; Ajayan, P. M. *Nano Res.* **2008**, *1*, 116–122.
(12) Datta, S. S.; Strachan, D. R.; Khamis, S. M.; Johnson, A. T. C. *Nano Lett.* **2008**, *8*, 1912–1915.
(13) Terrones, M. *Nature* **2009**, *458*, 845–846.
(14) Ouyang, Y.; Dai, H.; Guo, J. *Nano Res.* **2010**, *3*, 8–15.
(15) Jiao, L.; Zhang, L.; Ding, L.; Liu, J.; Dai, H. *Nano Res.* **2010**, *3*, 387–394.
(16) Wang, X.; Dai, H. *Nature Chem.* **2010**, *2*, 661–665.
(17) Cai, J.; Ruffieux, P.; Jaafar, R.; Bieri, M.; Braun, T.; Blankenburg, S.; Muoth, M.; Seitsonen, A. P.; Saleh, M.; Feng, X.; Mullen, K.; Fasel, R. *Nature* **2010**, *466*, 470–473.

(18) Jayasekera, T.; Mintmire, J. W. *Nanotechnology* **2007**, *18*, 424033.
(19) Areshkin, D. A.; White, C. T. *Nano Lett.* **2007**, *7*, 3253–3259.
(20) Liang, X.; Jung, Y.; Wu, S.; Ismach, A.; Olynick, D. L.; Cabrini, S.; Bokor, J. *Nano Lett.* **2010**, *10*, 2454–2460.
(21) Hohenberg, P.; Kohn, W. *Phys. Rev.* **1964**, *136*, B864.
(22) Kohn, W.; Sham, L. J. *Phys. Rev.* **1965**, *140*, A1133.
(23) Soler, J. M.; Artacho, E.; Gale, J. D.; Garcia, A.; Junquera, J.; Ordejon, P.; Sanchez-Portal, D. *J Phys: Condens. Matter* **2002**, *14*, 2745–2779.
(24) Perdew, J. P.; Ruzsinszky, A.; Csonka, G. I.; Vydrov, O. A.; Scuseria, G. E.; Constantin, L. A.; Zhou, X.; Burke, K. *Phys. Rev. Lett.* **2008**, *100*, 136406.
(25) Troullier, N.; Martins, J. L. *Phys. Rev. B* **1991**, *43*, 1993.
(26) Meunier, V.; Sumpter, B. G. *J. Chem. Phys.* **2005**, *123*, 024705–8.
(27) Cruz-Silva, E.; López-Urías, F.; Muñoz-Sandoval, E.; Sumpter, B. G.; Terrones, H.; Charlier, J.-C.; Meunier, V.; Terrones, M. *ACS Nano* **2009**, *3*, 1913–1921.
(28) Koskinen, P.; Malola, S.; Hakkinen, H. *Phys. Rev. B* **2009**, *80*, 073401–3.
(29) Lee, H.; Son, Y.; Park, N.; Han, S.; Yu, J. *Phys. Rev. B* **2005**, *72*, 174431.
(30) Slonczewski, J. C.; Weiss, P. R. *Phys. Rev.* **1958**, *109*, 272.
(31) White, C. T.; Li, J.; Gunlycke, D.; Mintmire, J. W. *Nano Lett.* **2007**, *7*, 825–830.
(32) Gunlycke, D.; White, C. T. *Phys. Rev. B* **2008**, *77*, 115116–6.
(33) Ohta, T.; Bostwick, A.; Seyller, T.; Horn, K.; Rotenberg, E. *Science* **2006**, *313*, 951–954.
(34) Dion, M.; Rydberg, H.; Schröder, E.; Langreth, D. C.; Lundqvist, B. I. *Phys. Rev. Lett.* **2004**, *92*, 246401.
(35) Romo-Herrera, J. M.; Terrones, M.; Terrones, H.; Meunier, V. *ACS Nano* **2008**, *2*, 2585–2591.
(36) Schwierz, F. *Nat. Nanotechnol.* **2010**, *5*, 487–496.
(37) Biró, L. P.; Lambin, P. *Carbon* **2010**, *48*, 2677–2689.